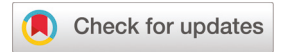
# Dalton Transactions



#### COMMUNICATION

View Article Online
View Journal | View Issue



**Cite this:** *Dalton Trans.*, 2020, **49**, 5429

Received 12th March 2020, Accepted 8th April 2020 DOI: 10.1039/d0dt00933d

rsc.li/dalton



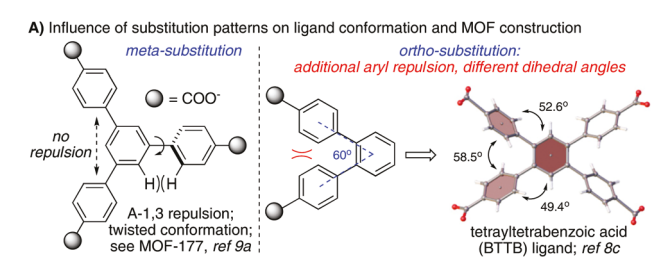
Jingyang Li, <sup>a</sup> Ying He, <sup>b</sup> Li Wang, <sup>©</sup> <sup>a</sup> Qinhe Pan, <sup>©</sup> <sup>c</sup> Zhiguang Song\* <sup>a</sup> and Xiaodong Shi <sup>©</sup> \* <sup>b</sup>

N-2-aryl-1,2,3-triazole derivatives were synthesized as new ligand systems for the construction of photoluminescent active metalorganic frameworks (MOFs). Crystal structures revealed that the five-membered triazoles show an unsymmetrical conformation with the two C4,C5-substituted benzenes adopting a "twisted-planar" geometry. As a result, a MOF constructed from this ligand exhibited cross-layer interactions with improved water stability (at 100 °C for 24 hours). Furthermore, enhanced photoluminescence emissions were observed upon the formation of MOF structures ( $\phi$  up to 30%), suggesting the potential applications of these photoactive porous materials through this new ligand design.

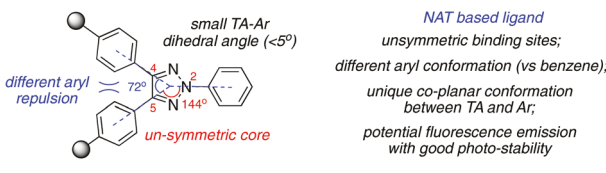
The past two decades have witnessed the fast growth of porous materials research.<sup>1</sup> Due to their large surface areas, tunable pore sizes, diverse geometries and accessible functional sites, porous materials have shown promising applications in various research fields, including gas molecule storage, chemical catalysis and molecular sensing.<sup>2</sup> As a very important class of porous materials, metal-organic frameworks (MOFs) have gained increasing attention in current chemicals and materials research.3 Although many well-developed molecular scaffolds with well-defined geometries have been reported in the past two decades, new building blocks with alternative binding patterns are always welcome and desirable since they could offer new coordination modes with potential interesting functionalities.4 Herein, we report N-2-aryl-1,2,3-triazole derivatives as linkers for the construction of metal-organic frameworks with significantly improved water stability, enhanced luminescence emission and selective CO2 adsorption.

Over the past decade, our group has been working on the development of 1,2,3-triazoles as building blocks for important chemical, material and biological applications.5 With success in discovering several new synthetic methods for the effective preparation of 1,2,3-triazole derivatives, our group first reported the strong fluorescence emission associated with N-2-aryl-1,2,3-triazoles (NATs).6 Moreover, X-ray crystal structures revealed a co-planar conformation between the triazoles and N-2-aryl rings, which could account for the observed strong photoemission. With continued interest in developing new chemical platforms for materials and biological research, we focus our attention on the potential application of these new molecular scaffolds in the construction of porous materials. In this manuscript, we report the first two MOF structures obtained from ligands based on the NAT core, NAT-MOF-1 and NAT-MOF-2.

As shown in Scheme 1A, multi-carboxylate ligands have been widely used for MOF construction through the COO-coordination with various metal cations.<sup>8</sup> For example, the 1,3,5-tri-aryl-benzoic acid ligand has been used for the prepa-



B) This work: construction of MOFs based on N-2-aryl-triazole (NAT), a new ligand core



**Scheme 1** (A) Benzene-core ligands for MOF construction. (B) NAT as the core structure for MOF construction.

<sup>&</sup>lt;sup>a</sup>State Key Laboratory of Supramolecular Structure and Materials, College of Chemistry, Jilin University, Changchun, Jilin 13002, China. E-mail: szg@jlu.edu.cn <sup>b</sup>Department of Chemistry, University of South Florida, 4202 E. Fowler Avenue, Tampa, Florida 33620, USA. E-mail: xmshi@usf.edu

<sup>&</sup>lt;sup>c</sup>Key Laboratory of Advanced Materials of Tropical Island Resources, Hainan University, Haikou 570228, P. R. China

<sup>†</sup>Electronic supplementary information (ESI) available. CCDC 1974068 and 1974069. For ESI and crystallographic data in CIF or other electronic format see DOI: 10.1039/D0DT00933D

Communication **Dalton Transactions** 

ration of MOF-177.9 Certainly, ligand conformation will greatly influence the overall binding pattern and final MOF topology.10 For benzene-based ligands, two general conformation concerns are (A) the binding angle between coordination sites and (B) the dihedral angle between the two adjacent aryl groups. 11 For the bis-benzene system, twisted conformation is observed in almost all cases due to the strong A-1,3 repulsion between the two benzene rings. 12 Interestingly, although some examples have been reported in the literature, MOFs prepared from ligands with 1,2-substituted benzene structures are much less compared with the 1,3-substituted analogues. 13 This is likely due to the smaller coordination angle (60° for 1,2-subs vs. 120° for 1,3-subs), which may cause increased steric hindrance toward metal cation coordination.<sup>14</sup>

Compared with popular benzene-core ligands, the NAT ligand has a very different conformation from the following perspectives. First, the two C4,C5-substituted groups show a larger binding angle (72°), which might lead to the preferred aryl group conformation with different overall repulsions. Meanwhile, the triazole ring and N-2-aryl ring adopted a coplanar conformation by avoiding the A-1,3 repulsion. More importantly, while the N-1-aryl triazole showed almost no fluorescence emission, manyN-2-aryl derivatives are good fluorophores exhibiting strong emission in the UV/blue light region.<sup>15</sup> All these unique structural features initiated our interest in exploring whether NATs can be used as ligands for preparation of MOFs with interesting new functions. To the best of our knowledge, there are few triazole based MOF structures reported so far and no NAT based MOF has ever been reported.<sup>16</sup> This is likely due to the challenges associated with the synthesis of ligands and structural control.<sup>17</sup> With recent success in triazole synthesis and functionalization, we prepared two NAT based ligands, L1 and L2 (Fig. 1A), and applied them for MOF construction under various metal binding conditions.

Using ligand L1, (4,4'-(2-phenyl-1,2,3-triazole-4,5-diyl)dibenzoic acid (TADA), with no carboxylate on the N2-phenyl group on triazole (Fig. 1B), NAT-MOF-1 was obtained under solvothermal conditions by dissolving Zn(NO<sub>3</sub>)<sub>2</sub>·6H<sub>2</sub>O and L1 (2:1) in solvents (1:1 DMF: MeOH) and heating at 85 °C for 72 hours. The FT-IR spectra (Fig. S2a†) of the resulting MOF revealed the disappearance of the carboxylic acid groups at around 2998 cm<sup>-1</sup> and the symmetric and the asymmetric stretching of the carboxylate groups at 1414 cm<sup>-1</sup> and 1529 cm<sup>-1</sup>. Fortunately, a crystal was successfully grown with its structure revealing a di-nuclear paddle-wheel secondary building unit (SBU) that consists of two Zn atoms binding to four L1 at approximately 90° with two dimethyl ether molecules coordinated on the top (Fig. 1C). The packing of unit cells along the c axes and a fragment of NAT-MOF-1 along the c axes showing fitted pores are also revealed in Fig. 1E and 1F, respectively.

Treating NAT ligand L2, 4,4',4"-(2*H*-1,2,3-triazole-2,4,5-triyl) tribenzoic acid (TATA), under similar solvothermal conditions gave NAT-MOF-2. The FT-IR spectra showed the characteristic band of the coordinated carboxylate groups at 1377 and

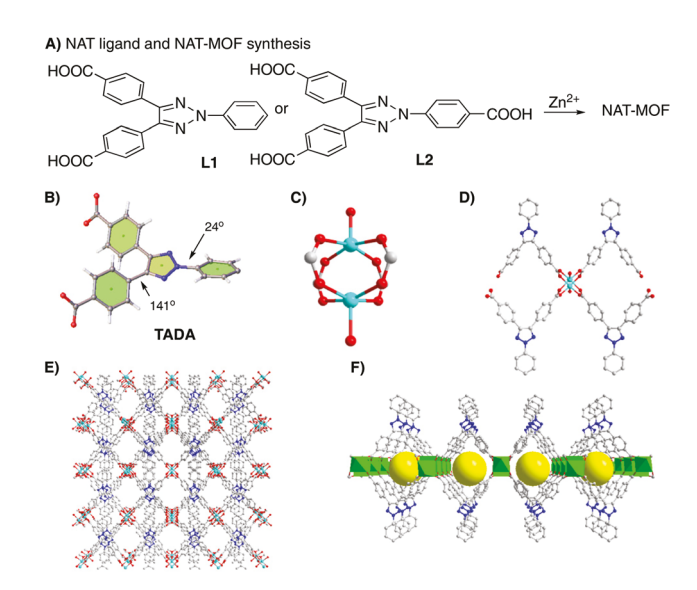


Fig. 1 NAT-MOF synthesis and crystal structure of NAT-MOF-1: (A) ligand and the general MOF synthetic route; (B) NAT ligand L1 (TADA); (C) Zn paddle-wheel SBU; (D) connectivity between TADA and paddlewheel SBU; (E) view of NAT-MOF-1 along the c axes; (F) view of a fragment of NAT-MOF-1 along the c axes showing fitted pores.

1606 cm<sup>-1</sup> (Fig. S2b†). The broad band at 2991 cm<sup>-1</sup> for carboxylic acid stretching disappeared, indicating the binding with metal cations. The crystal structure of NAT-MOF-2 was also successfully obtained as shown in Fig. 2.

The crystal structure of NAT-MOF-2 demonstrated a highly interpenetrated framework. Each repeating unit is composed of seven Zn(II) ions and four NAT ligands L2 (Fig. 2B and C). Zinc ions including Zn1, Zn2, Zn3, Zn4 and Zn7 compose a Zn<sub>5</sub> unit while the vertices of the network are connected by Zn5 and Zn6 in the horizontal direction and Zn3 and Zn7 connect the interlayers with a C5-substituted carboxylate group to give structural extension along the vertical directions, affording the interpenetrated networks. Interestingly, with the

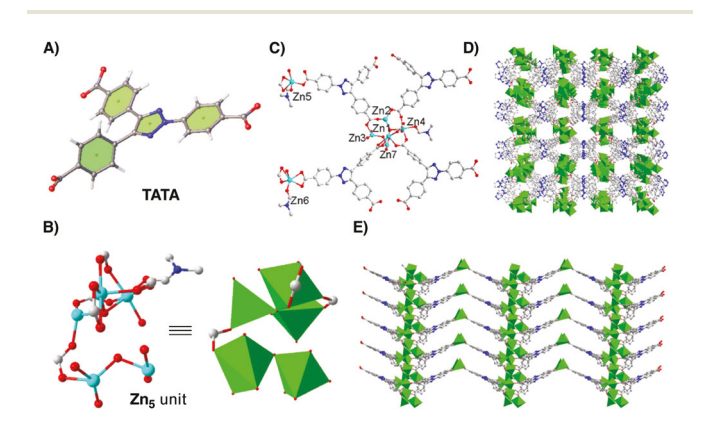


Fig. 2 Crystal structure and structural components of NAT-MOF-2: (A) triazole based linker L2; (B) central coordination environments of the Zn<sub>5</sub> unit: (C) overall coordination environments between ligand TATA and Zn(II) ions; (D) view of NAT-MOF-2 along the c and (E) b axes respectively.

**Dalton Transactions** Communication

highly unsymmetrical NAT core, the overall NAT-MOF-2 structure resembles a "roof tile" alignment. As shown in the crystal structure, this tile-like interpenetrated network is formed by the penetration of both horizontal and vertical directions. The stacking of tiles was assembled through the formation of the Zn<sub>5</sub> unit located in the middle of the tile. Meanwhile, due to the highly unsymmetrical factor of the crystal structure and unsymmetrical Zn5 unit coordination environments along the vertical direction in the center, there are four different conformations of L2 from the repeating units. To be specific, the dihedral angles between the NAT and carboxylate groups and the binding angles (107°-164°) of carboxylates from N-2 and C-4 positions resembling the basic layer of the tile structure appear to be unique in general. Interestingly, the binding modes for these two NAT-MOFs are dramatically different, which highlighted the importance of conformation control of these newly developed unsymmetrical NAT ligands. The powder X-ray diffraction (PXRD) spectra of both NAT-MOFs were collected. The diffraction patterns of the tested samples and the calculated data from crystal structure were compared (Fig. S1†). With the structures of both NAT-MOFs confirmed by X-ray, we set out to explore the influence of different topologies on the functions of the resulting MOF materials.

Unlike typical di-aryl compounds, one unique property of the NAT ligand is the co-planar conformation between the triazole and N-2 aryl rings. Our group has previously demonstrated that N-2-aryl triazoles could exhibit a strong fluorescence, while the N-1 isomer shows almost no emission. As a new class of small molecule organic fluorophores, NATs have some unique advantages, including luminescence efficiency, high thermal stability, good accessibility and easy modification.<sup>18</sup> However, during our previous studies, the emission efficiency was significantly reduced when introducing a carboxylate group on the N-2-aryl position. This is likely due to the various relaxation pathways (i.e. vibrational and rotational) typically associated with the carboxylate groups, which quenched the photo-excitation state. Considering that carboxylate will have a more locked conformation in MOF complexes over the free ligand, one could rationalize that improved fluorescence emission might be achieved upon MOF formation. To verify this hypothesis, the solid-state photoluminescence emissions of both ligands and MOFs were measured. As expected, the dramatic increase of fluorescence intensity was obtained for both NAT-MOFs over non-coordinated ligands (Fig. 3).

First, compared with non-substituted NAT compounds, the carboxylate group caused the reduction of photoemission, especially on the N-2-aryl position. While the N-2-phenyl ligand L1 (TADA) still shows luminescence emission in the solid state with a reduced quantum yield ( $\Phi$ ) of 13.8%, the dramatic quenching effect was observed with the N-2-benzoylic acid ligand L2 (TATA,  $\Phi = 0.59\%$ ). This is consistent with our previous report that the actual fluorophore in NAT is the N-2aryl moiety. Upon the formation of MOF structures, a significant increase of emission intensity was obtained for both

Stage	$\lambda_{ex}$	$\lambda_{\text{em}}$	Stokes	φ (0/\	nsity
	(nm)	(nm)	shift	Ф (%)	-L Inte
Ligand L1	355	381	26	14	pezil
NAT-MOF-1	336	377	41	31	dorma
Ligand L2	361	390	29	<1	-
NAT-MOF-2	363	382	19	17	

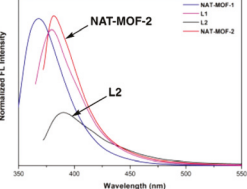


Fig. 3 Enhanced fluorescence emission upon the NAT-MOFs.

**NAT-MOF-1** ( $\Phi = 30.8\%$ ) and **NAT-MOF-2** ( $\Phi = 17.5\%$ ). This emission enhancement could be attributed to Zn-O coordination, which significantly reduced the possibility of excitation state relaxation, along with plausible  $\pi$ - $\pi$  stacking between adjacent aromatic moieties. This result is exciting since it suggests the great potential of these new MOF materials for photoactivation related applications.

Compared with benzene-based ligands, another interesting feature of the triazole-based ligand is the larger coordination angle between substituted groups at C4 and C5 positions (vs. 1,2substituted benzene). Clearly, this different binding angle will influence MOF topology as seen in the X-ray crystal structures.

The stability of MOFs in water plays a crucial role in the potential application of porous materials in the aqueous environment. 19 Generally, water stability depends on the steric effects of the ligand and strength of metal-ligand coordination.20 Therefore, solvent and moisture stability was also tested with these new type NAT-MOFs by comparing the PXRD data of the MOF samples upon soaking in a variety of solvents, including MeOH, acetonitrile, DCM and water. Although NAT-MOF-1 showed poor stability in organic solution, it demonstrated a relatively good stability in aqueous solution. As shown in Fig. 4, even after being immersed in boiling water for 24 hours, NAT-MOF-1 maintained most of its crystalline framework with several changes in diffraction angle signals. In contrast, NAT-MOF-2 presented a complete destructive breakdown of its porous framework as almost no signals were observed in the PXRD spectra.

For porous materials, gas sorption capacity and selectivity are certainly important factors to be evaluated. The CO2 adsorption data were collected at 195 K to examine the porosity of these NAT-MOFs (Fig. 5A).

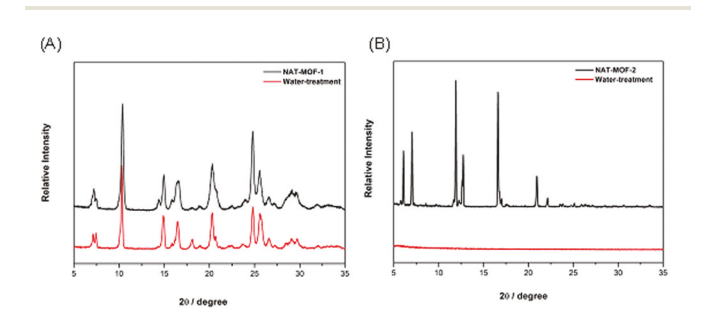


Fig. 4 Water stability of NAT-MOF-1 (A) and NAT-MOF-2 (B) evaluated

Communication **Dalton Transactions** 

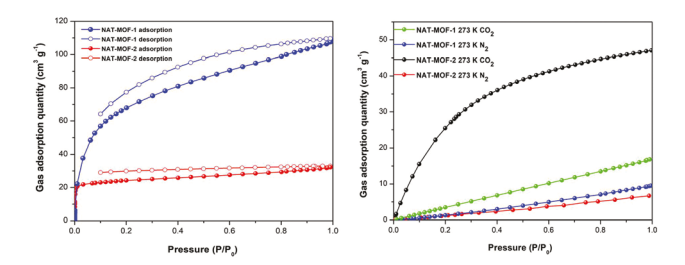


Fig. 5 (A) CO<sub>2</sub> sorption of NAT-MOF-1 and NAT-MOF-2 at 195 K. (B) CO2 and N2 sorption isotherms of NAT-MOF-1 and NAT-MOF-2 at 273 K.

Both frameworks exhibit reversible type-I isotherm adsorption features, in which the gas molecules present a sharp adsorption at relatively low pressure  $(P/P_0 < 0.1)$  which reaches a plateau subsequently. Desorption hysteresis loops were observed for both frameworks, which could be ascribed to the existence of mesopores and inevitable interactions between N atoms from 1,2,3-triazole backbones and oxygen from CO2 molecules. The Brunauer-Emmett-Teller (BET) and Langmuir surface area were calculated to be 216 m<sup>2</sup> g<sup>-1</sup> and 313 m<sup>2</sup> g<sup>-1</sup> for NAT-MOF-1 and 69 m<sup>2</sup> g<sup>-1</sup> and 96 m<sup>2</sup> g<sup>-1</sup> for NAT-MOF-2. NAT-MOF-1 showed higher BET surface areas over NAT-MOF-2 likely due to the size of micropores caused by higher dV/dw and highly symmetric structures. As a result, NAT-MOF-1 showed a maximum N<sub>2</sub> uptake of 9.5 cm<sup>3</sup> g<sup>-1</sup>, which is higher than a  $N_2$  uptake of 6.7 cm<sup>3</sup> g<sup>-1</sup> for NAT-MOF-2 at 273 K (Fig. 5B). The total pore volumes of 0.12 cm $^3$  g $^{-1}$  (NAT-MOF-2) and 0.52 cm<sup>3</sup> g<sup>-1</sup> (NAT-MOF-1) were estimated from the Horvath-Kawazoe calculation (Fig. S4†).

Notably, carbon dioxide (CO<sub>2</sub>) capture and storage (CCS) is of importance due to environmental concerns associated with growing atmospheric CO2 emissions caused by use of fossil fuels.<sup>21</sup> To evaluate the CO<sub>2</sub> uptake performances of these new MOFs, CO2 adsorption isotherms were collected for the activated samples at 273 K, as shown in Fig. 5(B). The results revealed a maximum adsorption of CO<sub>2</sub> of 17 cm<sup>3</sup> g<sup>-1</sup> and 47 cm<sup>3</sup> g<sup>-1</sup> at 273 K for NAT-MOF-1 and NAT-MOF-2, respectively. The value of CO<sub>2</sub>/N<sub>2</sub> selectivity was obtained using Ideal solution adsorbed theory (IAST) with a good correlation factor  $(R^2 > 0.999)$ . In general, nitrogen atoms in the organic linker and  $\pi$ -stacking could increase the CO<sub>2</sub> adsorption capacity.<sup>22</sup> Although the CO2 adsorption selectivity was modest (4.8, Fig. S5†), the fact that CO<sub>2</sub> can be adopted in this simple framework highlighted the polarized porous nature associated with the unique 1,2,3-triazole building blocks for CO<sub>2</sub> adsorption. In addition, the higher adsorption of NAT-MOF-2 compared to NAT-MOF-1 is presumably due to the extra carboxylate in L2 which results in more dipole-dipole interactions despite the interpenetrating framework. It is expected that further modification of this simple and easy-access structure could be done with improved adsorption ability and selectivity.

In conclusion, we reported herein the investigation of N-2aryl-1,2,3-triazole derivatives as ligands for the construction of MOF materials. Compared with widely applied benzene-based

linkers, NATs offer several unique features, including excellent fluorescence emission, co-planar conformation and larger binding angles at C4 and C5 positions. Two new metalorganic frameworks (NAT-MOFs) were successfully obtained upon coordination with Zn and their structures have been fully characterized by single crystal X-ray and PXRD. Some interesting properties have been revealed for these NAT-MOFs, including dramatically enhanced photoluminescence emission and selective CO2 adsorption. Overall, these studies not only set up a solid foundation for the design principle for the development of new porous materials using the NAT core, but also demonstrate the possibility of constructing new functional NAT-MOFs with good photoactivity. These studies are currently ongoing in our lab and will be reported in due course.

### Conflicts of interest

There are no conflicts to declare.

## Acknowledgements

We are grateful to NSF (CHE-1665122), Jilin Province (20170307024YY, 20190201080JC) for financial support.

#### Notes and references

- 1 (a) O. M. Yaghi, M. O'Keeffe, N. W. Ockwig, H. K. Chae, M. Eddaoudi and J. Kim, Nature, 2003, 423, 705-714; (b) M. E. Davis, Nature, 2002, 417, 813-821.
- 2 (a) R. B. Getman, Y. S. Bae, C. E. Wilmer and R. Q. Snurr, Chem. Rev., 2012, 112, 703-723; (b) H. Zhou, J. R. Long and O. M. Yaghi, Chem. Rev., 2012, 112, 673-674; (c) Y. Zhao, S. Qi, Z. Niu, Y. Peng, C. Shan, G. Verma, L. Wojtas, Z. Zhang, B. Zhang, Y. Feng, Y. Chen and S. Ma, J. Am. Chem. Soc., 2019, 141, 14443-14450.
- 3 D. Feng, W. Chung, Z. Wei, Z. Gu, H. Jiang, Y. Chen, D. J. Darensbourg and H. Zhou, J. Am. Chem. Soc., 2013, 135, 17105-17110.
- 4 M. Eddaoudi, J. Kim, N. Rosi, D. Vodak, J. Wachter, M. O'Keeffe and O. M. Yaghi, *Science*, 2002, **295**, 469–472.
- 5 (a) R. Cai, X. Ye, Q. Sun, Q. He, Y. He, S. Ma and X. Shi, ACS Catal., 2017, 7, 1087-1092; (b) X. Ye, C. Xu, L. Wojtas, N. Akhmedov, H. Chen and X. Shi, Org. Lett., 2016, 18, 2970-2973.
- 6 (a) Y. Zhang, X. Ye, J. L. Petersen, M. Li and X. Shi, J. Org. Chem., 2015, 80, 3664-3669; (b) D. Wang, X. Ye and X. Shi, Org. Lett., 2010, 12, 2088-2091.
- 7 Y. Liu, W. Yan, Y. Chen, J. L. Petersen and X. Shi, Org. Lett., 2008, 10, 5389-5392.
- 8 (a) T. He, Y. Zhang, H. Wu, X. Kong, X. Liu, L. Xie, Y. Dou and J. Li, ChemPhysChem, 2017, 18, 3245-3252; (b) B. Gómez-Lor, E. Gutiérrez-Puebla, M. Iglesias, M. A. Monge, C. Ruiz-Valero and N. Snejko, Chem. Mater.,

Dalton Transactions Communication

- 2005, 17, 2568–2573; (c) J. R. Karra, Y. Huang and K. S. Walton, *Cryst. Growth Des.*, 2013, 13, 1075–1081.
- 9 (a) H. K. Chae, D. Y. Siberio-Pérez, J. Kim, Y. Go, M. Eddaoudi, A. J. Matzger, M. O'Keeffe and O. M. Yaghi, *Nature*, 2004, 427, 523–527; (b) Y. Zhang, H. Furukawa, N. Ko, W. Nie, H. Park, S. Okajima, K. E. Cordova, H. Deng, J. Kim and O. M. Yaghi, *J. Am. Chem. Soc.*, 2015, 137, 2641–2650.
- 10 D. Zhao, D. J. Timmons, D. Yuan and H. Zhou, Acc. Chem. Res., 2011, 44, 123–133.
- 11 (a) F. Lundvall, P. D. C. Dietzel and H. Fjellvag, *Acta Crystallogr., Sect. E: Crystallogr. Commun.*, 2016, 72, 328–330; (b) M. E. Braun, C. D. Steffek, J. Kim, P. G. Rasmussen and O. M. Yaghi, *Chem. Commun.*, 2001, 2532–2533.
- 12 D. Bara, C. Wilson, M. Mörtel, M. M. Khusniyarov, S. Ling, B. Slater, S. Sproules and R. S. Forgan, *J. Am. Chem. Soc.*, 2019, 141, 8346–8357.
- 13 B. Li, H. Wen, Y. Cui, W. Zhou, G. Qian and B. Chen, Adv. Mater., 2016, 28, 8819–8860.
- 14 (a) J. Pang, S. Yuan, J. Qin, C. Liu, C. Lollar, M. Wu, D. Yuan, H. Zhou and M. Hong, J. Am. Chem. Soc., 2017, 139, 16939–16945; (b) Y. Wang, L. Feng, W. Fan, K. Wang, X. Wang, X. Wang, K. Zhang, X. Zhang, F. Dai, D. Sun and H. Zhou, J. Am. Chem. Soc., 2019, 141, 6967–6975.
- 15 (a) Q. Lai, Q. Liu, K. Zhao, C. Shan, L. Wojtas, Q. Zheng,
  X. Shi and Z. Song, *Chem. Commun.*, 2019, 55, 4603-4606;
  (b) Q. Lai, Q. Liu, Y. He, K. Zhao, C. Y. Wei, L. Wojtas,

- X. Shi and Z. Song, Org. Biomol. Chem., 2018, 16, 7801-7805.
- (a) P. Li, X. Wang, L. Liu, J. Lim, R. Zou and Y. Zhao, J. Am. Chem. Soc., 2016, 138, 2142–2145; (b) X. Guo, X. Feng, T. Han, S. Wang, Z. Lin, Y. Dong and B. Wang, J. Am. Chem. Soc., 2014, 136, 15485–15488; (c) P. Li, X. Wang and Y. Zhao, Coord. Chem. Rev., 2019, 380, 484–518; (d) V. Gupta and S. K. Mandal, Chem. Eur. J., 2020, 26, 2658–2665.
- 17 S. Sengupta, H. Duan, W. Lu, J. L. Petersen and X. Shi, *Org. Lett.*, 2008, **10**, 1493–1496.
- 18 J. Kalisiak, K. B. Sharpless and V. V. Fokin, *Org. Lett.*, 2008, **10**, 3171–3174.
- 19 (a) H. A. Lara-García, M. R. Gonzalez, J. H. González-Estefan, P. Sánchez-Camacho, E. Lima and I. A. Ibarra, *Inorg. Chem. Front.*, 2015, 2, 442–447; (b) J. Canviet, A. Fateeva, Y. Guo, B. Coasne and D. Farrusseng, *Chem. Soc. Rev.*, 2014, 43, 5594–5617.
- 20 E. Sánchez-González, J. R. Álvarez, R. A. Peralta, A. Campos-Reales-Pineda, A. Tejeda-Cruz, E. Lima, J. Balmaseda, E. González-Zamora and I. A. Ibarra, ACS Omega, 2016, 1, 305–310.
- 21 J. Li, R. J. Kuppler and H. Zhou, Chem. Soc. Rev., 2009, 38, 1477–1504.
- 22 (a) R. Boulmène, M. Prakash and M. Hochlaf, *Phys. Chem. Chem. Phys.*, 2016, 18, 29709–29720; (b) L. H. Xie and M. P. Suh, *Chem. Eur. J.*, 2013, 19, 11590–11159.